bridge.[1,40] The increased sturdiness of the heterocyclic-bridged polydeckers is central to their appeal as models for the study of delocalization in extended metal-π stacks.

The magnetic properties and ESR spectra of a number of odd-electron triple deckers with $C_3B_2R_5$ bridges were reported by Edwin and co-workers.[5] The 29-e$^-$ complex $Cp_2FeCo(C_3B_2R_5)^+$ was shown to have a $^2E_{2g}$ ground state analogous to that of Cp_2Fe^+ (when proper allowance is made for reduction of symmetry upon substitution of $C_3B_2R_5^{3-}$ for $C_5H_5^-$).

Our 29-e$^-$ systems $RuRu^+$ and $CuRu^+$ are isoelectronic with the above FeCo cation, and we draw a similar conclusion about the electronic ground state. [In fact, in these complexes, the e_2'' level is expected to split into a close-lying a' ($d_{x^2-y^2}$) and a'' (d_{xy}) pair owing to the reduction of symmetry from D_{5d}. A single-crystal ESR study would be necessary to distinguish between the two possibilities.] Although the Mossbauer spectra of the FeCo cation suggested a large amount of Fe character in the SOMO, a Co hyperfine splitting in the low-field g component was observed (ca. 50×10^{-4} cm^{-1}). We find a similar feature in the ESR spectrum of $CoRu^+$. These observations suggest that, in 29-e$^-$ triple deckers of Co and Fe (or Ru), the half-filled orbital is distributed over both metals, with the *dominant* contribution being from the iron-group metal.

The 31-e$^-$ heterodinuclear complexes may also be compared: the present $CoRu^-$ with $Cp_2FeCo(C_3B_2R_5)^-$ and $Cp_2CoNi(C_3B_2R_5)^+$.[5] In all three cases, the observation of an ESR g component with a value of less than g_e eliminates a d_{z^2} SOMO[41] and argues strongly for d_{xz} or d_{yz}, descendant from the e_1' pair. However, the cobalt splittings vary greatly in this set of complexes. The iron-group complexes $CoRu^-$ and $Cp_2FeCo(C_3B_2R_5)^-$ have a large low-field splitting of ca. 120×10^{-4} cm^{-1}, whereas the same splitting in $Cp_2CoNi(C_3B_2R_5)^+$ is only 27×10^{-4} cm^{-1}. A tentative conclusion is that although these triple deckers show spin-delocalization when possessing odd-electron counts, the distribution of the unpaired electron is dependent on nuclear properties of the metals, and possibly on the properties of the bridging or capping ligands. Further investigation of these possibilities is warranted.

If these molecules are viewed as pentagonal bipyramidal clusters, our results also confirm two key predictions of Johnston and Mingos[42] for such systems, namely that (1) the HOMO/LUMO spacing of 30-e$^-$ clusters is small, allowing electron counts in excess of 30, and (2) the LUMO of the 30-e$^-$ system will always be doubly degenerate (or nearly so, depending on symmetry), whereas the HOMO may either be doubly degenerate (e-type) or singly degenerate (a-type).[42]

Finally, the observation of completely delocalized $RuRu^+$ and $CoRu^+$ cations is encouraging with respect to the construction of electroactive (and possibly magnetoactive) polymers incorporating carborane-bridged triple-decker or tetra-decker sandwich units.

Acknowledgment. We are grateful to the National Science Foundation for support of this research at both the University of Vermont (Grant CHE 86-03728 and 91-16332) and the University of Virginia (Grant CHE 90-22713).

(40) For stable 27-e$^-$ complexes with bridging P_5 ligands, see: (a) Scherer, O. J.; Schwalb, J.; Wolmershaeuser, G.; Kaim, W.; Gross, R. *Angew. Chem., Int. Ed. Engl.* **1986**, *25*, 363. (b) Scherer, O. J.; Schwalb, J.; Swarowsky, H.; Womershaeuser, G.; Kaim, W.; Gross, R. *Chem. Ber.* **1988**, *121*, 443.

(41) Reference 37, pp 110 ff.

(42) Johnston, R. L.; Mingos, D. M. P. *J. Chem. Soc., Dalton Trans.* **1987**, 647.

Mechanism of Formation of C-C Bonds in the Ring Opening and Coupling of Thiophene by $(C_5Me_5)Rh(C_2H_4)_2$

William D. Jones* and R. Martin Chin

Contribution from the Department of Chemistry, University of Rochester, Rochester, New York 14627. *Received June 1, 1992*

Abstract: Thermolysis of $(C_5Me_5)Rh(C_2H_4)_2$ in the presence of thiophene leads to the formation of the new product, $[(C_5Me_5)Rh]_2[1,2,3,4\text{-}\eta^4\text{-}5,6,7,10\text{-}\eta^4\text{-}S(CH)_8S]$. The related reaction with dibenzothiophene leads first to the sulfur-bridged C-S-inserted cis dimer $[(C_5Me_5)Rh(\mu_2\text{-}\eta^2\text{-}SC_{12}H_8)]_2$ and then to the trans dimer of the same formula. These complexes have been structurally characterized, with the cis complex crystallizing in monoclinic space group $C2/c$ with a = 16.323 (6) Å, b = 15.355 (5) Å, c = 14.646 (5) Å, β = 92.61 (3)°, Z = 4, and V = 3666.8 (4.1) Å^3. The trans isomer crystallizes in triclinic space group $P\bar{1}$, with a = 9.995 (3) Å, b = 10.290 (2) Å, c = 11.230 (2) Å, α = 112.02 (1)°, β = 97.99 (2)°, γ = 114.66 (2)°, Z = 1, and V = 911.2 (1.1) Å^3. The reaction of $(C_5Me_5)Rh(C_2H_4)_2$ with 2-methoxythiophene is found to lead to the monomer $(C_5Me_5)\overline{Rh[C(OMe)=CHCH=CHS]}$, which is in equilibrium with the corresponding cis and trans sulfur-bridged dimers. The rate of cleavage of the cis dimer to give the monomer at 22 °C is 3.12 (12) $\times 10^{-3}$ s^{-1}. The rate of cleavage of the trans dimer to give the monomer at 22 °C is 1.25 (4) $\times 10^{-5}$ s^{-1}. Equilibrium parameters for the cis $\rightleftharpoons$ monomer equilibrium are $\Delta H°$ = 7.0 (0.7) kcal/mol and $\Delta S°$ = 19 (2) eu. Equilibrium parameters for the trans $\rightleftharpoons$ monomer equilibrium are $\Delta H°$ = 10.4 (0.7) kcal/mol and $\Delta S°$ = 28 (2) eu. An X-ray structural determination of the cis dimer shows the complex to crystallize in triclinic space group $P\bar{1}$, with a = 8.335 (4) Å, b = 10.096 (3) Å, c = 19.832 (5) Å, α = 89.54 (2)°, β = 78.49 (3)°, γ = 67.97 (3)°, Z = 2, and V = 1511.9 (2.1) Å^3. The trans dimer crystallizes in triclinic space group $P\bar{1}$, with a = 10.814 (3) Å, b = 10.816 (5) Å, c = 16.301 (4) Å, α = 84.79 (3)°, β = 88.15 (2)°, γ = 68.79 (3)°, Z = 2, and V = 1770.1 (2.2) Å^3. These structures are discussed with regard to the mechanism of the C-C bond forming reaction.

Introduction

The reactions of thiophenes with transition metals as models for studying the hydrodesulfurization of petroleum have become of increased interest over the past few years.[1] A variety of coordination modes of thiophene have been exhibited and structurally characterized,[2] and reactions in which the ring has been cleaved by attack of external reagents have been reported.[3] More

(1) Angelici, R. J. *Acc. Chem. Res.* **1988**, *21*, 387-394. Friend, C. M.; Roberts, J. T. *Acc. Chem. Res.* **1988**, *21*, 394-400.

(2) Angelici, R. J. *Coord. Chem. Rev.* **1990**, *105*, 61-76. Rauchfuss, T. B. *Prog. Inorg. Chem.* **1991**, *39*, 259-329.

0002-7863/92/1514-9851$03.00/0

recently, the simple insertion of an unsaturated rhodium[4] or iridium[5] metal center into the thiophene C–S bond has also been reported.

In the case of $[(C_5Me_5)Rh(PMe_3)]$, coordination of the sulfur of thiophene was shown to precede the insertion of the metal into the C–S bond (eq 1). Coordination to the π system in an η^2 fashion led to C–H bond oxidative addition. In comparison, the iridium species was found to insert into the C–S bond following η^4 coordination in $(C_5Me_5)Ir(\eta^4$-dimethylthiophene) and was catalyzed by added base (eq 2). The latter iridium complex is formally 16 electron and achieves an 18-electron count by delocalization of a sulfur lone pair into the metallathiabenzene ring, resulting in a planar structure. In contrast, the rhodium complex achieves an 18-electron configuration through the presence of a PMe_3 ligand, and consequently the lack of electron delocalization results in a bent, localized diene structure.

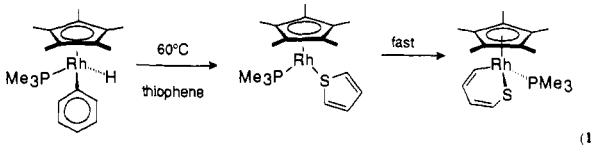

(1)

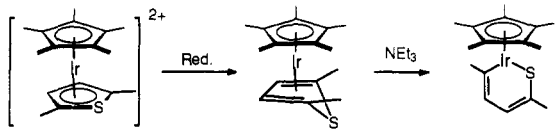

(2)

Also of related interest is the complex $(C_5Me_5)Rh(\eta^4$-$C_4Me_4S)$ studied by Rauchfuss and co-workers. This molecule showed no tendency to undergo a similar C–S insertion reaction, although thermolysis of trimeric $[(C_5Me_5)Rh]_3(\eta^4,\eta^1$-$SC_4Me_4)_2$ did give a product in which rhodium had inserted into the C–S bond (eq 3).[6] The reaction of $(C_5Me_5)Co(C_2H_4)_2$ with thiophene led to a similar bimetallic ring-opened product that was structurally characterized (eq 4).[7]

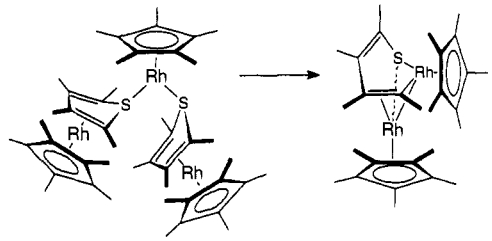

(3)

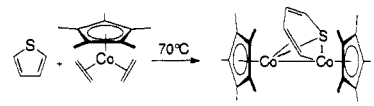

(4)

In the present study, we attempted to examine a rhodium complex that would insert into the C–S bond of thiophene but would then have a labile ligand in place of the PMe_3 group. $(C_5Me_5)Rh(C_2H_4)_2$, which is known to be active in C–H bond activation,[8] proved to be just such a complex, although we were surprized to find that, while C–S cleavage does indeed occur, a facile unprecedented C–C bond forming reaction occurs concomitant with the C–S cleavage.[9]

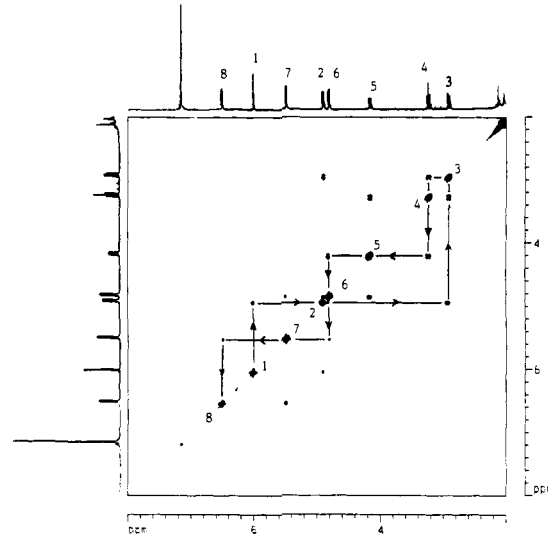

Figure 1. ^1H–^1H COSY spectrum of **1**.

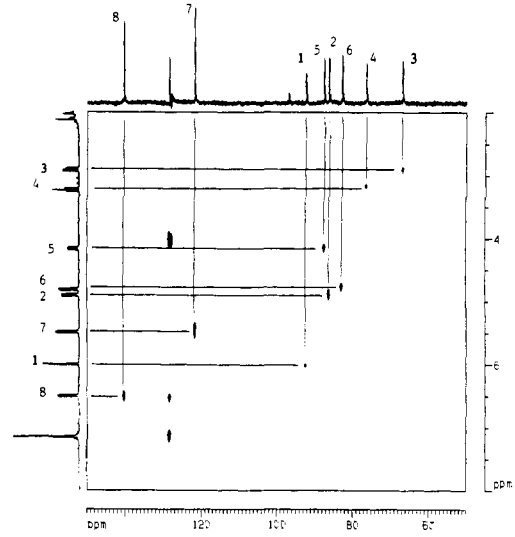

Figure 2. ^1H–^{13}C HETCOR spectrum of **1**.

Results

Reaction of $(C_5Me_5)Rh(C_2H_4)_2$ with Thiophene. Heating a benzene solution of $(C_5Me_5)Rh(C_2H_4)_2$ with a 20-fold excess of thiophene at 100 °C results in the slow formation of free ethylene and a product containing two distinct C_5Me_5 ligands as evidenced by ^1H NMR spectroscopy.[10] In addition, eight distinct multiplets of area 1 H each are seen in the δ 3–7 ppm region of the spectrum. A ^1H–^1H COSY spectrum revealed that each of the six most upfield resonances was coupled only to two nearest neighbors and that the two remaining downfield resonances were coupled to only one nearest neighbor, indicating that an asymmetric 8-carbon

(3) Spies, G. H.; Angelici, R. J. *Organometallics* **1987**, *6*, 1897–1903. Hachgenei, J. W.; Angelici, R. J. *J. Organomet. Chem.* **1988**, *355*, 359–378. Ogilvy, A. E.; Draganjac, M.; Rauchfuss, T. B.; Wilson, S. R. *Organometallics* **1988**, *7*, 1171–1177. Hübener, P.; Weiss, E. *J. Organomet. Chem.* **1977**, *129*, 105–115.

(4) Jones, W. D.; Dong, L. *J. Am. Chem. Soc.* **1991**, *113*, 559–564. Dong, L.; Duckett, S. B.; Ohman, K. F.; Jones, W. D. *J. Am. Chem. Soc.* **1992**, *114*, 151–160.

(5) Chen, J.; Daniels, L. M.; Angelici, R. J. *J. Am. Chem. Soc.* **1990**, *112*, 199–204.

(6) Luo, S.; Skaugset, A. E.; Rauchfuss, T. B.; Wilson, S. R. *J. Am. Chem. Soc.* **1992**, *114*, 1732–1735.

(7) Jones, W. D.; Chin, R. M. *Organometallics* **1992**, *11*, 2698–2700.

(8) Seiwell, L. P. *J. Am. Chem. Soc.* **1974**, *96*, 7134–7135.

(9) A preliminary account of this work has appeared; see: Chin, R. M.; Jones, W. D. *Angew. Chem., Int. Ed. Engl.* **1992**, *31*, 357–358.

(10) The reaction proceeds to only ~50–70% completion after 15 h, and further heating results in little additional reaction. Degassing the sample to remove ethylene does not allow further conversion. Running the reaction in neat thiophene does not produce any of the C–C coupled product, nor does the bis-ethylene complex diminish. Addition of NEt_3 has no effect on the rate of product formation.

$(CH)_8$ array was present (Figure 1). A ^{13}C–^1H HETCOR spectrum revealed that, of the eight carbons, the six most upfield resonances showed a doublet coupling to rhodium, but the two most downfield resonances were singlets and were in the region expected for free olefinic carbon atoms (Figure 2). Furthermore, the six carbons attached to rhodium were at one end of the $(CH)_8$ chain. The product was formulated as the C–S ring-opened C–C coupled product **1** on the basis of this NMR data (eq 5). Subsequent isolation of a single small crystal provided sufficient data for an X-ray structure to be determined confirming this geometry (Figure 3), but the small quantity of data prevented a high-quality structure determination.[9]

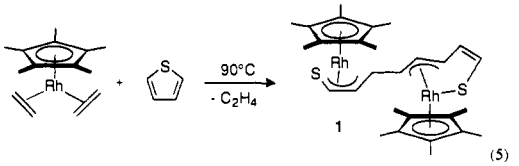

(5)

Reaction of $(C_5Me_5)Rh(C_2H_4)_2$ with 2-deuteriothiophene results in the formation of **1**-d_4, in which the resonances at δ 6.503, 6.009, 4.165, and 3.245 are diminished in intensity by one-half, indicating that deuteriums are located only on carbons 1, 4, 5, and 8 (eq 6). This distribution is consistent with coupling of the two α-carbons of thiophene following cleavage of the C–S bond.

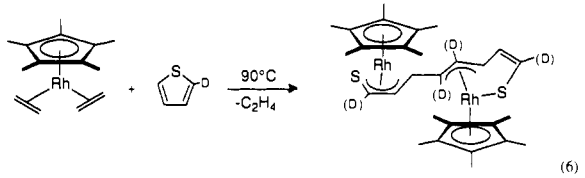

(6)

In an attempt to look for an intermediate, a solution of $(C_5Me_5)Rh(C_2H_4)_2$ in benzene containing thiophene was irradiated (310–380 nm) for 6 h. A small amount of a new product with a C_5Me_5 doublet resonance at δ 1.504 was observed in the ^1H NMR spectrum. In addition, four multiplets were seen at δ 11.843 (ddd, J = 9.2, 6.3, 1.6 Hz, 1 H), 9.082 (dd, J = 8.7, 6.8 Hz, 1 H), 8.256 (ddd, J = 9.4, 7.1, 1.3 Hz, 1 H), and 7.575 (ddd, J = 9.0, 7.1, 1.3 Hz, 1 H), suggesting the formation of $(C_5Me_5)Rh[CH{=}CHCH{=}CHS]$ (eq 7). The dimer **1** was also observed as the major product, and upon standing at room temperature the resonances for the intermediate decreased as those for **1** increased.

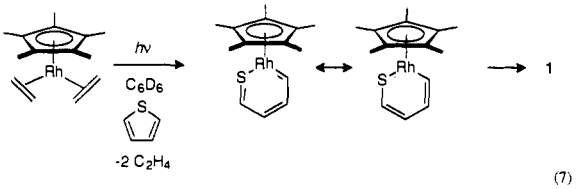

(7)

Reaction of $(C_5Me_5)Rh(C_2H_4)_2$ with Dibenzothiophene. Heating a solution of $(C_5Me_5)Rh(C_2H_4)_2$ with an excess of dibenzothiophene in benzene at 100 °C results in the formation of an orange solution. ^1H NMR examination of the sample shows the production of a single new product containing a single C_5Me_5 resonance and eight distinct olefinic multiplets. Further heating of the sample for 2–3 days results in the formation of a red crystalline precipitate. The ^1H NMR spectrum of this material in CD_2Cl_2 solvent also shows a single C_5Me_5 resonance and eight distinct olefinic multiplets.

The red product was easily isolated by continued heating, and a single-crystal X-ray structure of the product shows it to be a symmetrical trans dimer structure in which the $(C_5Me_5)Rh$ fragment has inserted into the C–S bond of the dibenzothiophene following loss of both ethylenes and in which the insertion adduct has undergone a head-to-tail dimerization of the Rh–S bonds, leaving the two C_5Me_5 rings on opposite sides of the Rh_2S_2 square planar core (eq 8). The complex *trans*-**2** sits on a crystallographic

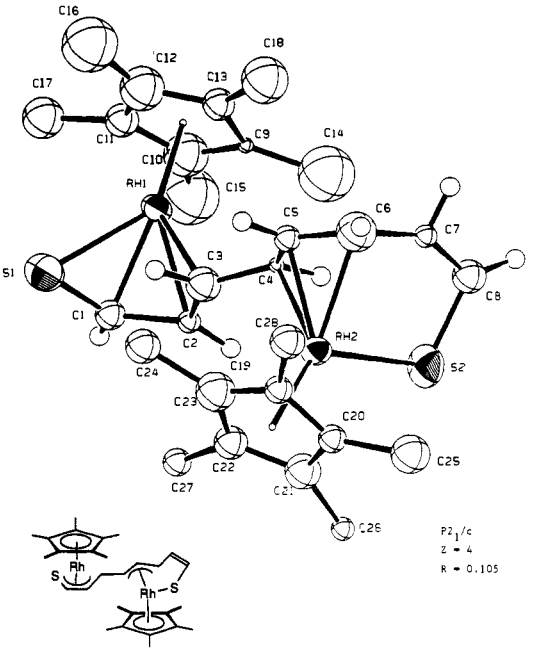

Figure 3. ORTEP plot of **1**. The C_5Me_5 groups were refined as rigid groups with all atoms isotropic except rhodium and sulfur.

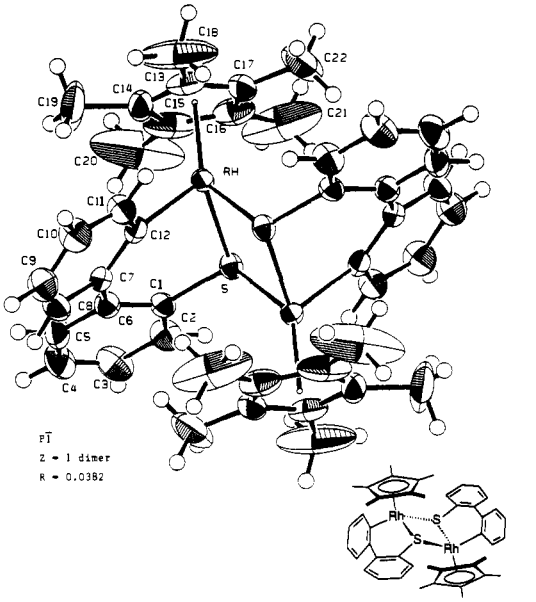

Figure 4. ORTEP drawing of *trans*-**2**. Ellipsoids are shown at the 50% probability level.

center of inverstion and consequently involves coupling of both R and S stereochemistries at the rhodium center to give an R/S dimer. An ORTEP drawing is shown in Figure 4.

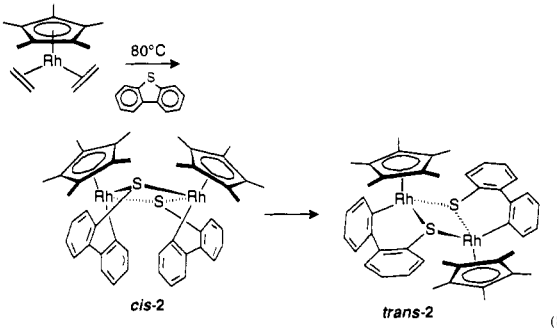

(8)

Isolation of the orange product proved possible by stopping the reaction at the point where this species is maximized. A sin-

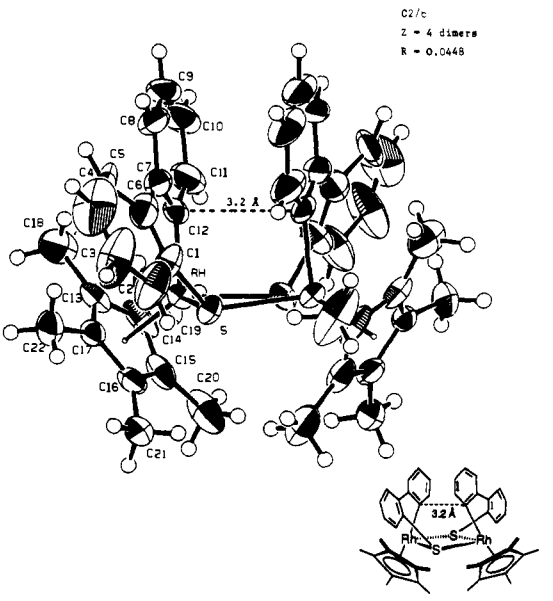

Figure 5. ORTEP drawing of *cis*-2. Ellipsoids are shown at the 50% probability level. The C12–C12′ nonbonding distance is 3.2 Å.

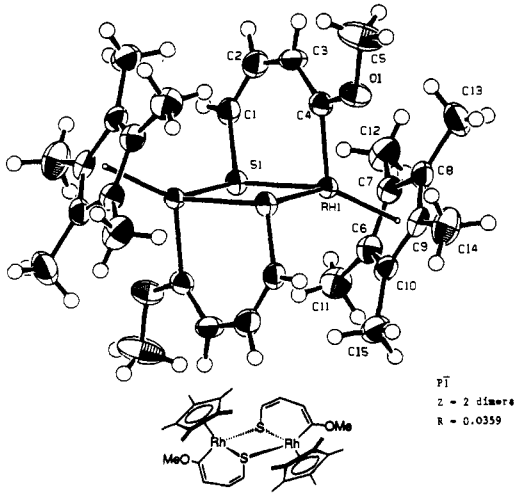

Figure 6. ORTEP drawing of *trans*-3. Ellipsoids are shown at the 50% probability level.

gle-crystal X-ray structure determination showed this material to be the cis dimer of **2**, with the two C_5Me_5 ligands on the same side of the Rh_2S_2 core. Complex *cis*-**2** sits on a 2-fold crystallographic axis, and it is worthwhile noting that the C12–C12′ nonbonding distance is only 3.2 Å. The centrosymmetric space group $C2/c$ requires that both R and S rhodium centers be present, but now they join to give both R/R and S/S pairs. An ORTEP drawing is shown in Figure 5.

Reaction of $(C_5Me_5)Rh(C_2H_4)_2$ with 2-Methoxythiophene. Heating a solution of $(C_5Me_5)Rh(C_2H_4)_2$ with an excess of 2-methoxythiophene in benzene at 100 °C results in the formation of a purple solution which shows evidence for the presence of three distinct species by ^1H NMR spectroscopy in a 16:4:1 ratio. The major species could not be isolated and displays resonances at δ 6.85 (d, J = 8.8 Hz, 1 H), 7.58 (t, J = 8.8 Hz, 1 H), and 9.02 (dd, J = 8.6, 6.8 Hz, 1 H), as well as a C_5Me_5 resonance at δ 1.64 and a methoxy resonance at 3.75. The two minor species each displayed C_5Me_5 and MeO resonances, as well as olefinic multiplets in the δ 3–7 range of the ^1H NMR spectrum. Upon concentration of the solution by removal of the solvent under vacuum, the purple solution became deep red until finally dark red crystals precipitated. Careful separation of two colors of crystals (orange and dark red) allowed isolation of the two minor products. Dissolution of each of these complexes in cold (<−40 °C) toluene-d_8 allowed NMR characterization of the products.

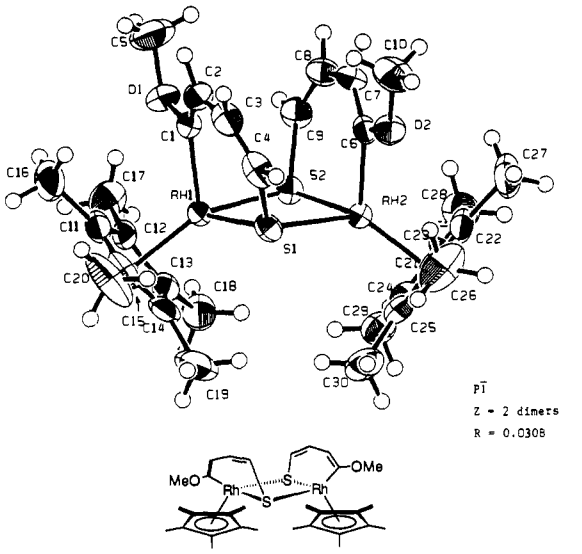

Figure 7. ORTEP drawing of *cis*-3. Ellipsoids are shown at the 50% probability level. The C12–C12′ nonbonding distance is 3.88 Å.

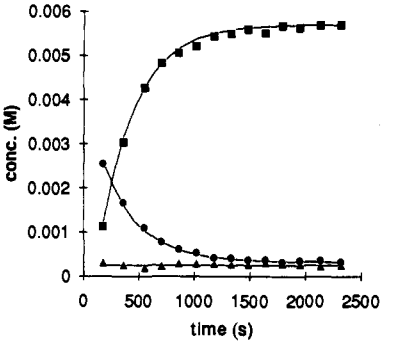

Figure 8. Distribution of species during the approach to equilibrium by *cis*-3 at 22 °C in C_6D_6: ● = *cis*-3; ▲ = *trans*-3; ■ = 4.

Furthermore, single-crystal X-ray structural determinations were carried out for each type of crystal, showing them to be the cis and trans dimers (*cis*-**3** and *trans*-**3**) in which the $(C_5Me_5)Rh$ fragment had again inserted into the C–S bond of the thiophene adjacent to the methoxy group (eq 9). ORTEP drawings are shown in Figures 6 and 7. Once again, the cis complex shows a close C1–C6 nonbonding distance of only 3.88 Å.

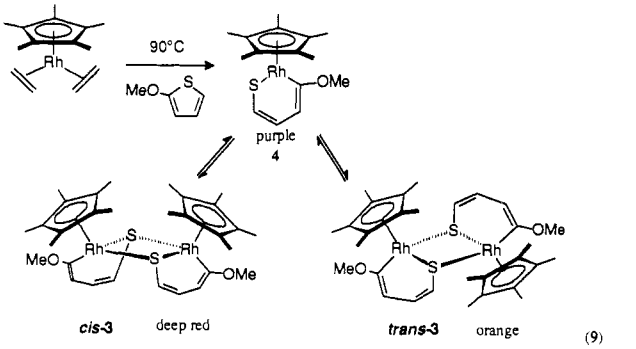

(9)

The major species of this reaction was consequently assigned as the monomer $(C_5Me_5)Rh[C(OMe)=CHCH=CHS]$ (**4**). Dimerization of the monomer is induced upon concentration of solution, which allows isolation of only *cis*-**3** and *trans*-**3**. Furthermore, this dimerization was found to be reversible. Dissolution of crystals of *cis*-**3** in toluene-d_8 solution at 22 °C results in the rapid ($\tau_{1/2}$ = 3.7 min, k = 3.12 (3) × 10^{-3} s^{-1}) generation of monomer **4**, with equilibrium being reached between these two species in about 1 h (Figure 8). Equilibration with *trans*-**3** occurs on a much slower time scale, requiring days at room temperature.

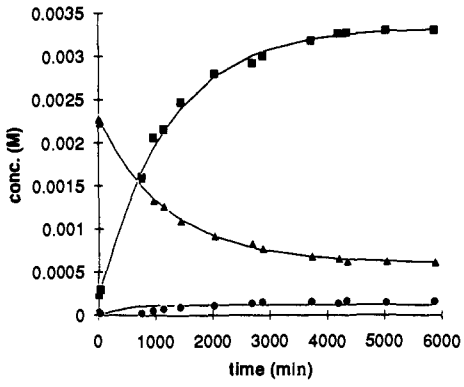

Figure 9. Distribution of species during the approach to equilibrium by *trans*-**3** at 22 °C in C_6D_6: ● = *cis*-**3**; ▲ = *trans*-**3**; ■ = **4**.

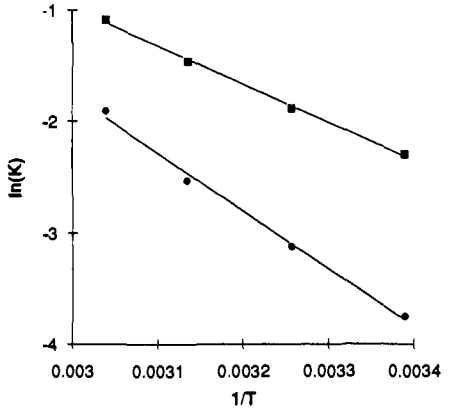

Figure 10. van't Hoff plot for the equilibrium between *trans*-**3** and **4** (■) and between *cis*-**3** and **4** (●).

Similarly, isolated crystals of *trans*-**3** could be dissolved in toluene-d_8 and the approach to equilibrium with the monomer monitored by ^1H NMR spectroscopy at 22 °C. The rate of approach is much slower ($\tau_{1/2}$ = 15.4 h, k = 1.25 (4) × 10^{-5} s^{-1}), so that now equilibration between monomer **4** and *cis*-**3** occurs as the amount of *trans*-**3** diminishes (Figure 9).

The temperature dependence of these equilibria was measured by ^1H NMR spectroscopy by holding the temperature of the sample constant for 2–3 days at temperatures between 22 and 56 °C. Plots of ln (K_{eq}) vs $1/T$ were linear (Figure 10), giving equilibrium thermodynamic parameters for *trans*-**3** ⇌ **4** of $\Delta H°$ = 10.4 (0.7) kcal/mol and $\Delta S°$ = 28 (2) eu. For *cis*-**3** ⇌ **4**, $\Delta H°$ = 7.0 (0.7) kcal/mol and $\Delta S°$ = 19 (2) eu.

Discussion

The reaction of $(C_5Me_5)Rh(C_2H_4)_2$ with thiophenes in all cases leads to products in which the rhodium has inserted into the C–S bond, as summarized in Scheme I. The reaction would be expected to proceed by way of initial ethylene loss followed by coordination of sulfur and insertion into the C–S bond in analogy to the mechanism delineated for $[(C_5Me_5)Rh(PMe_3)]$.[4] This C–S insertion adduct probably readily loses ethylene, however, as the Rh(III) species would not be expected to bind the π acceptor ethylene ligand as tightly as the Rh(I) starting material.[11] The vacant site on the metal can be filled by donation from the lone pair on a sulfur from a second complex, leading to the formation of the square Rh_2S_2 core. These complexes are observed for both the dibenzothiophene and 2-methoxythiophene insertions, but not for thiophene itself.

The formation of cis and trans dimers from the monomer requires some discussion. In the case of dibenzothiophene, no

Scheme I

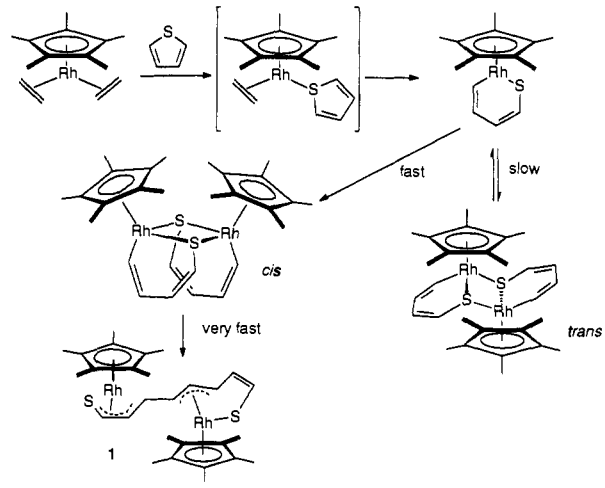

monomer intermediate is observed, and the dimer *cis*-**2** is seen as the kinetic product resulting from *R*/*R* and *S*/*S* coupling. Upon further heating, the dimer dissociates back to the monomer and more slowly couples in an *R*/*S* fashion to give the thermodynamically preferred *trans*-**2**. It is not clear at this time as to whether the monomer is bent, and therefore has *R* and *S* forms, or whether the monomer is planar and the chirality is induced along the pathway to dimer formation. The latter view is probably correct, as the related mononuclear iridium derivatives isolated and structurally characterized by Angelici and co-workers are planar.[5]

No C–C coupling product is observed with dibenzothiophene, as formation of a C–C bond between C12 and C12′ would destroy the aromaticity of two benzene rings. The crystal structure of *cis*-**2** does show the close approach (3.2 Å) of these two carbons, however. Also of importance is the orientation of the ring-opened thiophene fragments, which shows the p orbitals on the carbons that would be coupled pointing directly toward each other. This geometry is thought to be a model of the transition state for the thiophene C–C coupling reaction. The proximity and orientation of the carbon atoms in the thiophene analog of *cis*-**2** should be similar, but the C–C coupling now readily occurs to give the $S(CH)_8S$ chain. Unbridging of the sulfur atoms and re-coordination of the polyolefin chain produces **1** as the thermodynamic product. Such a coupling does not occur in *cis*-**2** as there would be a penalty for disrupting the aromaticity of two benzene rings.

In the case of the dimer formation with 2-methoxythiophene, the monomer **4** can now be observed in equilibrium with *cis*-**3** and *trans*-**3**. Insertion into the more hindered side of this substrate was unexpected. The stability of this monomer can be accounted for in terms of the delocalized resonance forms for the 16-electron insertion adduct. One of these forms formally contains a methoxycarbene moiety, which lowers the energy of this monomer compared to the dibenzothiophene case (eq 10). At the typical concentrations used in these experiments (~0.003 M), the monomer is the major species in solution.

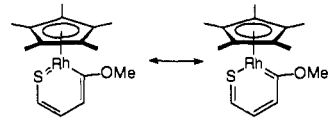

(10)

The ability to isolate *cis*-**3** and *trans*-**3** allowed the determination of the barriers for equilibration with the monomer. Plots of ln ($[dimer]_t$ − $[dimer]_{eq}$) were linear, giving unimolecular rate constants for the respective conversions. The barriers $\Delta G^‡$ determined at 22 °C in this fashion are indicated in Scheme II. Equilibration of the mixture of *trans*-**3**, *cis*-**3**, and **4** at different temperatures gives the equilibrium thermodynamic parameters separating these species. Since monomer/dimer equilibria are involved, free energies will be relative to a standard state, in this

(11) An alternative mechanism for the formation of the insertion product would be to form $(C_5Me_5)Rh(\eta^4\text{-}C_4H_4S)$, analogous to Rauchfuss' $(C_5Me_5)Rh(\eta^4\text{-}C_4Me_4S)$ and Angelici's $(C_5Me_5)Ir(\eta^4\text{-}C_4Me_2H_2S)$, prior to the C–S insertion. The requirement of base catalysis in this mechanism might explain the slowing of the rate after ~50% completion.

Table I. X-ray Data for *cis*-2, *trans*-2, *cis*-3, and *trans*-3

	trans-2	*cis*-2	*trans*-3	*cis*-3
chemical formula	$Rh_2S_2C_{44}H_{46}$	$Rh_2S_2C_{44}H_{46}$	$Rh_2S_2O_2C_{30}H_{42}{\cdot}SC_5H_3OCH_3$	$Rh_2S_2O_2C_{30}H_{42}$
cryst syst	triclinic	monoclinic	triclinic	triclinic
space group (No.)	$P\bar{1}$ (2)	$C2/c$ (15)	$P\bar{1}$ (2)	$P\bar{1}$ (2)
Z	1	4	2	2
a, Å	9.995 (3)	16.323 (6)	10.814 (3)	8.335 (4)
b, Å	10.290 (2)	15.355 (5)	10.816 (5)	10.096 (3)
c, Å	11.230 (2)	14.646 (5)	16.301 (4)	19.832 (5)
α, deg	112.02 (1)	90	84.79 (3)	89.54 (2)
β, deg	97.99 (2)	92.61 (3)	88.15 (2)	78.49 (3)
γ, deg	114.66 (2)	90	68.79 (3)	67.97 (3)
vol, Å^3	911.2 (1.1)	3666.8 (4.1)	1770.0 (2.2)	1511.9 (2.1)
ρ_{calcd}, g cm^{-3}	1.54	1.53	1.54	1.55
temp, °C	−40	−40	−20	−20
2θ range, deg	4–50 ($+h,\pm k,\pm l$)	4–50 ($+h,+k,\pm l$)	4–50 ($+h,\pm k,\pm l$)	4–48 ($+h,\pm k,\pm l$)
intensities (unique, R_i)	3403 (3201, 0.038)	3400 (3271, 0.050)	6578 (6219, 0.030)	5129 (4759, 0.034)
intensities > $3\sigma(F^2)$	2596	1919	4087	3750
no. of params varied	217	217	388	325
μ, cm^{-1}	10.31	10.25	11.19	12.31
abs corr	differential	differential	differential	differential
range trans. factors	0.903–1.087	0.73–1.19	0.92–1.10	0.90–1.16
$R(F_o)$	0.0382	0.0448	0.0359	0.0308
$R_w(F_o)$	0.0430	0.0496	0.0390	0.0398
goodness of fit	1.46	1.57	1.26	1.60

Scheme II

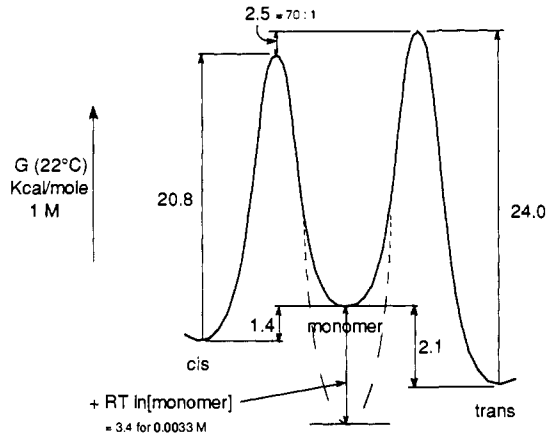

case chosen as 1 M.[12] Under the experimental conditions of [**4**] = ~0.0033 M, the free energy of **4** must be lowered by RT ln [**4**] (3.4 kcal/mol) in order to properly reflect the distribution of species, as shown in Scheme II by the dotted line. From this diagram, the kinetic selectivity of the monomer for forming *cis*-**3** vs *trans*-**3** can be determined to be 70:1 ($\Delta\Delta G^{\ddagger}$ = 2.5 kcal/mol). The more rapid equilibration of the monomer with the cis dimer can also be seen, as the barrier is lower for this process.

The reaction of $(C_5Me_5)Rh(C_2H_4)_2$ with thiophene proceeds directly to the C—C coupled dithiooctatetraene product. The initially formed intermediate $(C_5Me_5)\overline{Rh[CH{=}CHCH{=}CHS]}$ is analogous to the iridium complexes isolated by Angelici and co-workers with 2-methylthiophene and 2,5-dimethylthiophene.[5] ^{1}H NMR resonances for this intermediate were detected at δ 11.843, 9.082, 8.256, and 7.575, which compare with the values reported by Angelici and co-workers for the 2-methylthiophene insertion complex. The rhodium complex, however, quickly dimerizes and C—C couples. Once the C—C bond is formed from the cis dimer, unbridging of the sulfur atoms and coordination of the unbound olefins result in the formation of **1**. The unsymmetrical nature of **1** is somewhat unexpected, as one can envision the formation of a symmetrical species in which $(C_5Me_5)Rh$ is coordinated to the four atoms at each end of the $S(CH)_8S$ chain, leaving the free double bond in the center. As the rhodium is expected to be capable of migrating up and down the chain at the temperature at which **1** is formed,[13] the observed geometry must be the result of a thermodynamic preference for coordination to six adjacent carbons. No evidence for dynamic interconversion of the independent $(C_5Me_5)Rh$ centers is seen upon heating the sample to 90 °C.

The C–C bond formation involving the coupling of carbon atoms on adjacent metal centers is uncommon. It is perhaps most related to the coupling of dienes on palladium centers, which is believed to involve a reductive dimerization of butadiene.[14] While couplings of sp^2-hybridized carbons on a single metal center are common, couplings of carbon ligands on separate metals are less well documented.[15] Several polynuclear systems have been studied which show activities related to the chemistry presented here. Curtis has studied the reactions of a sulfur-bridged $Mo_2Co_2(\mu\text{-}S)_3$ cluster which extracts sulfur from thiophene to produce a $Mo_2Co_2(\mu_3\text{-}S)_4$ cluster plus small hydrocarbon products.[16] No intermediates were detected, however. Adams has examined reactions of $Os_3(CO)_{12}$ with a number of small cyclic sulfur compounds and has found ring-opened products containing bridging sulfur atoms.[17] Finally, Jensen has recently observed the insertion of a mononuclear palladium complex into a cyclic thioether, which then reductively eliminates to form a carbon–chlorine bond.[18]

The single-crystal X-ray structures of *trans*-**2**, *cis*-**2**, *trans*-**3**, and *cis*-**3** are the first of their type. Tables I and II compare the relevant central structural features. All complexes display alternating short–long–short bond distances around the thiophene ring, indicative of little metallathiabenzene character. The nonbonding rhodium–rhodium distances all lie around 3.5 Å, and the Rh–S bond holding the dimers together is slightly longer than the Rh–S bond within the metallathiacycle ring. The Rh–C_α distances of 2.01–2.05 Å are typical of Rh–sp^2-carbon bond lengths. Bond angles within the complexes are quite similar. There

(12) Benson, S. W. *Thermochemical Kinetics*; John Wiley and Sons: New York, 1976; p 8.

(13) Smith, A. K.; Maitlis, P. M. *J. Chem. Soc., Dalton Trans.* **1976**, 1773–1777.

(14) Tsuji, J. *Organic Synthesis with Palladium Complexes*; Springer-Verlag: Berlin, 1980.

(15) Collman, J. P.; Hegedus, L. S.; Norton, J. R.; Finke, R. G. *Principles and Applications of Organotransition Metal Chemistry*; University Science Books: Mill Valley, CA, 1987; p 333.

(16) Riaz, U.; Curnow, O.; Curtis, M. D. *J. Am. Chem. Soc.* **1991**, *113*, 1416–1417.

(17) Adams, R. D.; Chen, G.; Sun, S.; Wolfe, T. A. *J. Am. Chem. Soc.* **1990**, *112*, 868–869. Adams, R. D.; Pompeo, M. P. *Organometallics* **1990**, *9*, 1718–1720. Adams, R. D.; Pompeo, M. P. *Organometallics* **1990**, *9*, 2651–2653. Adams, R. D.; Pompeo, M. P. *J. Am. Chem. Soc.* **1991**, *113*, 1619–1626.

(18) Yamamoto, H. H.; Yap, G. P. A.; Jensen, C. M. *J. Am. Chem. Soc.* **1991**, *113*, 5060–5061.

Table II. Selected Distances (Å) and Angles (deg) in *trans*-**2**, *cis*-**2**, *trans*-**3**, and *cis*-**3**[a]

	trans-**2**	*cis*-**2**	*trans*-**3**[b]	*cis*-**3**[c]
		Bond Distances		
Rh_1–C_α	2.059 (5)	2.021 (7)	2.013 (6), 2.018 (6)	2.014 (5), 2.002 (5)
C_α–C_β	1.402 (7)	1.400 (13)	1.353 (8), 1.352 (9)	1.330 (7), 1.341 (7)
C_β–C_γ	1.484 (7)	1.556 (15)	1.440 (9), 1.46 (1)	1.433 (8), 1.449 (8)
C_γ–C_δ	1.415 (7)	1.407 (13)	1.330 (9), 1.318 (9)	1.339 (7), 1.320 (7)
S–C_δ	1.764 (5)	1.775 (8)	1.760 (6), 1.748 (6)	1.757 (5), 1.755 (5)
Rh_1–S	2.312 (2)	2.306 (2)	2.337 (2), 2.335 (2)	2.329 (2), 2.329 (2)
Rh_2–S	2.379 (2)	2.366 (2)	2.388 (2), 2.382 (2)	2.379 (2), 2.379 (2)
Rh_1–Rh_2	3.554 (2)	3.565 (2)	3.547 (1), 3.548 (2)	3.515 (1)
		Bond Angles		
Rh_1–S–Rh_2	98.48 (6)	99.47 (8)	97.32 (6), 97.53 (6)	96.59 (6), 96.61 (6)
Rh_1–C_α–C_β	128.4 (4)	126.6 (7)	129.0 (5), 128.7 (5)	129.4 (4), 130.0 (4)
C_α–C_β–C_γ	124.4 (4)	125.5 (8)	126.3 (6), 125.9 (6)	127.2 (5), 126.4 (5)
C_β–C_γ–C_δ	124.2 (4)	123.7 (9)	129.0 (6), 128.8 (6)	130.0 (5), 130.1 (5)
C_γ–C_δ–S	125.5 (4)	124.8 (8)	125.1 (5), 126.0 (5)	125.5 (4), 125.9 (4)
C_δ–S–Rh_1	107.6 (2)	108.2 (3)	107.9 (2), 107.4 (2)	109.2 (2), 109.2 (2)
S–Rh_1–C_α	89.8 (1)	91.2 (3)	90.7 (2), 90.7 (2)	92.7 (1), 92.6 (1)

[a] Distances and angles are listed using the atom scheme:

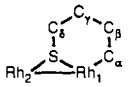

[b] Values are for the two independent halves of the molecule, each lying on a center of symmetry. [c] Values are for the two halves of the molecule, which lies in a general position.

are slight differences in the puckering of the metallathiacycle rings, in which the sulfur and four carbon atoms are coplanar with the rhodium lying out of the plane at angles of 21–31°. The two phenyl rings of the dibenzothiophene adducts show twisting about the C–C bond joining these rings of ~26–29°.

Conclusions

The ring opening of thiophene by insertion of a low-valent metal into the C–S bond is found to be quite general and can lead to C–C bond formation by a new route. Dimer formation by way of bridging sulfur atoms can lead to the juxtaposition of two metal carbon bonds with p orbitals properly oriented for C–C bond formation. The factors controlling the formation of the dimers (both cis and trans) have been elucidated, as have the factors influencing the stability of the monomeric C–S insertion adduct.

Experimental Section

General. All operations and routine manipulations were performed under a nitrogen atmosphere, either on a high-vacuum line using modified Schlenk techniques or in a Vacuum Atmospheres Corporation dri-lab. Tetrahydrofuran, benzene, and toluene were distilled from dark purple solutions of benzophenone ketyl. Benzene-d_6, THF-d_8, and toluene-d_8 were distilled under vacuum from dark purple solutions of benzophenone ketyl and stored in ampules with Teflon-sealed vacuum line adapters. $(C_5Me_5)Rh(C_2H_4)_2$ was prepared as previously reported.[19] Thiophenes were obtained from Aldrich Chemical Co. and were used as received.

All ^1H NMR spectra were recorded on a Bruker AMX400 NMR spectrometer. All chemical shifts are reported in ppm (δ) relative to tetramethylsilane and referenced to the chemical shifts of residual solvent resonances (C_6H_6, δ 7.15). Data were typically recorded with a digital resolution of 0.3 Hz. All temperatures for variable-temperature NMR spectroscopy were calibrated relative to the chemical shift differences in the NMR spectra of known standards (298–386 K, 80% ethylene glycol in DMSO-d_6; 228–298 K, 4% methanol in methanol-d_4). All kinetic plots and least-squares error analyses of rate data were done using Microsoft Excel. Analyses were obtained from Desert Analytics.

Preparation of $[(C_5Me_5)Rh]_2[1,2,3,4\text{-}\eta^4\text{-}5,6,7,10\text{-}\eta^4\text{-}S(CH)_8S]$. A solution of $(C_5Me_5)Rh(C_2H_4)_2$ (122 mg, 0.41 mmol) and thiophene (200 μL, 2.5 mmol) in 20 mL of benzene was freeze–pump–thaw degassed (3×) and heated in an ampule attached to a Teflon valve at 90 °C for 15 h. A ^1H NMR spectrum of an aliquot showed 30% conversion to product. The solvent was removed under vacuum, and the residue was dissolved in 45 mL of benzene and 200 μL of thiophene added. Heating for 24 h followed by removal of solvent showed 40% conversion (other experiments showed up to 70% conversion to product). Washing with hexane (5–10 mL) yielded pure red-black crystals of **1** (20 mg, 20% isolated yield): ^1H NMR (400 MHz, C_6D_6, 25 °C) δ 6.503 (dd, J = 5.5, 3.3 Hz, H_8), 6.009 (dt, J = 3.9, 1.0 Hz, H_1), 5.492 (dd, J = 6.4, 3.9 Hz, H_7), 4.900 (ddd, J = 8.0, 3.9, 2.0 Hz, H_2), 4.818 (dd, J = 6.8, 4.0 Hz, H_6), 4.165 (ddd, J = 11.3, 7.0, 1.0 Hz, H_5), 3.245 (t, J = 11.0 Hz, H_4), 2.915 (ddt, J = 11.0, 7.9, 1.3 Hz, H_3), 1.681 (s, C_5Me_5), 1.463 (s, C_5Me_5); $^{13}C\{^1H\}$ NMR (100 MHz, C_6D_6, 25 °C) δ 140.14 (s, H_8), 121.55 (s, H_7), 92.17 (d, J = 9.5 Hz, H_1), 87.46 (d, J = 6.0 Hz, H_2), 86.14 (d, J = 6.0 Hz, H_5), 82.69 (d, J = 12.1 Hz, H_6), 76.26 (d, J = 7.0 Hz, H_4), 66.70 (d, J = 10.2 Hz, H_3), 96.71 (d, J = 6.7 Hz, C_5Me_5), 96.82 (d, J = 5.7 Hz, C_5Me_5), 10.05 (s, C_5Me_5), 9.08 (s, C_5Me_5). Anal. Calcd (Found) for $Rh_2S_2C_{28}H_{38}$: C, 52.18 (52.17); H, 5.94 (5.74).

Observation of $(C_5Me_5)\overline{Rh[CH{=}CHCH{=}CHS]}$. A solution of $(C_5Me_5)Rh(C_2H_4)_2$ (0.034 M) and thiophene (0.31 M) in benzene-d_6 was irradiated (200 W Hg, λ = 310–380 nm) for 6 h. A ^1H NMR spectrum of the sample showed the formation of ethylene and a small amount (~3–4%) of a new product, assigned as the insertion adduct $(C_5Me_5)\overline{Rh[CH{=}CHCH{=}CHS]}$, as well as the C–C coupled product **1** (~10%): ^1H NMR (C_6D_6) δ 1.504 (s, 15 H), 11.843 (ddd, J = 9.2, 6.3, 1.6 Hz, 1 H), 9.082 (dd, J = 8.7, 6.8 Hz, 1 H), 8.256 (ddd, J = 9.4, 7.1, 1.3 Hz, 1 H), 7.575 (ddd, J = 9.0, 7.1, 1.3 Hz, 1 H).

Preparation of *cis*- and *trans*-$[(C_5Me_5)Rh(\mu\text{-}SC_{12}H_8)]_2$. $(C_5Me_5)Rh(C_2H_4)_2$ (100.7 mg, 0.342 mmol) and dibenzothiophene (206.5 mg, 1.12 mmol) were dissolved in 10 mL of benzene and placed in a Teflon-stopcocked ampule. The solution was degassed by three freeze–pump–thaw cycles. The yellow solution was heated at 100–110 °C for 24 h. Free ethylene and the solvent were completely removed under vacuum (10^{-4} mmHg), and the remaining solid was redissolved in 10 mL of benzene. The solution was heated for an additional 36 h, by which time the solution had turned black. The benzene was removed under vacuum, and the residue was washed with 3 × 5 mL of hexanes. A total of 49 mg of an orange-brown powder was isolated (34% combined yield of cis and trans isomers). The ^1H NMR spectrum showed a 4.3:1 ratio of cis:trans isomers. *cis*-$[(C_5Me_5)Rh(\mu\text{-}SC_{12}H_8)]_2$: ^1H NMR (CD_2Cl_2) δ 1.40 (s, 15 H), 6.12 (ddd, J = 7.6, 7.0, 1.6 Hz, 1 H), 6.49 (ddd, J = 7.7, 7.0, 1.3 Hz, 1 H), 6.58 (dd, J = 7.7, 1.4 Hz, 1 H), 6.71 (dd, J = 7.8, 1.4 Hz, 1 H), 6.92 (ddd, J = 7.5, 7.1, 1.4 Hz, 1 H), 7.12 (ddd, J = 8.0, 7.0, 1.4 Hz, 1 H), 7.31 (d, J = 8.1 Hz, 1 H), 7.49 (dd, J = 7.6, 1.5 Hz, 1 H). Anal. Calcd (Found) for $C_{44}H_{46}Rh_2S_2$: C, 62.56 (62.27); H, 5.49 (5.44). *trans*-$[(C_5Me_5)Rh(\mu\text{-}SC_{12}H_8)]_2$: ^1H NMR δ 0.93 (s, 15 H), 7.01 (ddd, J = 8.7, 7.1, 1.3 Hz, 1 H), 7.13 (m, 2 H), 7.24 (ddd, J = 8.4, 7.3, 1.4 Hz, 1 H), 7.56 (m, 2 H), 7.61 (dd, J = 8.1, 1.4 Hz, 1 H), 8.04 (m, 1 H). Anal. Calcd (Found) for $C_{44}H_{46}Rh_2S_2$: C, 62.56 (62.30); H, 5.49 (5.44).

Preparation of *cis*- and *trans*-$[(C_5Me_5)Rh(\mu\text{-}SC_4H_3OMe)]_2$. $(C_5Me_5)Rh(C_2H_4)_2$ (64.4 mg, 0.219 mmol) and 2-methoxythiophene (2 mL, 15.5 mmol) were dissolved in 100 mL of benzene and placed into a 250-mL Teflon-stopcock flask. The solution was heated at 90–100 °C for a total of 48 h. The solution was degassed every 12 h by removing approximately 5–10 mL of solvent under vacuum. The solvent was

(19) Maitlis, P. M.; Kang, J. W.; Moseley, K. *J. Chem. Soc. A* **1970**, 2875.

removed from the deep purple solution, and the brown residue was redissolved in 1–2 mL of hexanes and recrystallized at −35 °C. The solution was decanted to yield 30 mg of orange powdered *cis*-$[(C_5Me_5)Rh(\mu\text{-}SC_4H_3OMe)]_2$ and black-red crystalline *trans*-$[(C_5Me_5)Rh(\mu\text{-}SC_4H_3OMe)]_2$ (39% combined yield). *cis*-$[(C_5Me_5)Rh(\mu\text{-}SC_4H_3OMe)]_2$: ^{1}H NMR (toluene-$d_8$) δ 1.62 (s, 15 H), 3.66 (s, 3 H), 4.44 (m, 1 H), 5.63 (d, J = 7.8 Hz, 1 H), 6.49 (dd, J = 9.6, 8.4 Hz, 1 H). Anal. Calcd (Found) for $C_{30}H_{42}O_2Rh_2S_2$: C, 51.14 (51.06); H, 6.01 (5.88). *trans*-$[(C_5Me_5)Rh(\mu\text{-}SC_4H_3OMe)]_2$: ^{1}H NMR δ 1.49 (s, 15 H), 3.73 (s, 3 H), 4.32 (dt, J = 9.2, 2.0 Hz, 1 H), 5.64 (d, J = 7.4 Hz, 1 H), 6.74 (dd, J = 9.2, 7.2 Hz, 1 H). Anal. Calcd (Found) for $C_{30}H_{42}O_2Rh_2S_2$: C, 51.14 (51.04); H, 6.01 (6.05).

Generation of $(C_5Me_5)\overline{Rh[C(OMe)=CHCH=CHS]}$. $(C_5Me_5)Rh(C_2H_4)_2$ (1 mg, 0.003 mmol) and 2-methoxythiophene (6 μL, 0.04 mmol) were dissolved in 0.5 mL of C_6D_6 and placed in a resealable NMR tube. The yellow solution was heated at 100–110 °C for 2 days. A ^{1}H NMR spectrum of the resulting deep purple solution showed that the conversion to $(C_5Me_5)\overline{Rh[C(OMe)=CHCH=CHS]}$ was quantitative: ^{1}H NMR (C_6D_6) δ 1.64 (s, 15 H), 3.75 (s, 3 H), 6.85 (d, J = 8.8 Hz, 1 H), 7.58 (t, J = 8.8 Hz, 1 H), 9.02 (dd, J = 8.6, 6.8 Hz, 1 H).

Kinetics of Equilibration of *trans*-$[(C_5Me_5)Rh(\mu\text{-}SC_4H_3OMe)]_2$. *trans*-$[(C_5Me_5)Rh(\mu\text{-}SC_4H_3OMe)]_2$ (1.2 mg, 0.0017 mmol) was placed into a resealable NMR tube, and 0.7 mL of toluene-d_8 was condensed in at −78 °C. The sample was shaken at low temperature until all of the complex had gone into solution. The sample was warmed to room temperature by placing it in a water bath, and ^{1}H spectra were recorded until the reaction reached equilibrium. The cis:trans:monomer ratios were monitored by integrating the methoxy resonances.

Kinetics of Equilibration of *cis*-$[(C_5Me_5)Rh(\mu\text{-}SC_4H_3OMe)]_2$. *cis*-$[(C_5Me_5)Rh(\mu\text{-}SC_4H_3OMe)]_2$ (1.7 mg, 0.0024 mmol) was placed into a resealable NMR tube, and 0.7 mL of toluene-d_8 was condensed in at −78 °C. The sample was shaken at low temperature until all of the *cis*-$[(C_5Me_5)Rh(\mu\text{-}SC_4H_3OMe)]_2$ had gone into solution. The sample was warmed to room temperature by placing it in a water bath, and ^{1}H spectra were recorded until the reaction reached equilibrium. The cis:trans:monomer ratio was monitored by integrating the methoxy resonances.

Temperature Dependence of Equilibrium Ratios of *cis*-3:*trans*-3:Monomer. The sample (from the above kinetic experiments) was held at a particular temperature for 1–2 days, and a ^{1}H spectrum was recorded. After 12 h another ^{1}H spectrum was recorded to ensure that the cis:trans:monomer ratio was unchanged.

X-ray Structural Determination of *trans*-$[(C_5Me_5)Rh(\mu_2\text{-}\eta^2\text{-}SC_{12}H_8)]_2$. A red prism of compound **2** was grown in an NMR tube and mounted with epoxy on a glass fiber. Preliminary cell determination was made with 25 centered reflections with values of χ between 0 and 70°. Routine data collection of one hemisphere of data was undertaken on the primitive triclinic cell as indicated in Table I. The Molecular Structure Corporation TEXSAN analysis software package was used for data reduction and solution.[20] Patterson map solution of the structure to locate the rhodium atom, followed by expansion of the structure with the program DIRDIF, revealed all nonhydrogen atoms. The molecule was found to sit on a crystallographic center of inversion, such that only $^1/_2$ of one molecule was found in the asymmetric unit. Following isotropic refinement, an absorption correction was applied using the program DIFABS. Full-matrix least-squares anisotropic refinement of the non-hydrogen atoms (with hydrogens attached to carbons in idealized positions) was carried out to convergence. Fractional coordinates are given in the supplementary material and selected distances and angles in Table II.

X-ray Structural Determination of *cis*-$[(C_5Me_5)Rh(\mu_2\text{-}\eta^2\text{-}SC_{12}H_8)]_2$. The data collection, solution, and refinement of this molecule proceeded similarly to that of the trans isomer, except that the complex crystallized in monoclinic space group $C2/c$ with four dimer molecules per unit cell. Solution and refinement were carried out as above, with the molecule lying on a crystallographic 2-fold axis of rotation. Fractional coordinates are given in the supplementary material and selected distances and angles in Table II.

X-ray Structural Determination of *trans*-$[(C_5Me_5)Rh(\mu\text{-}SC_4H_3OMe)]_2$. The data collection, solution, and refinement of this molecule proceeded as above, except that the complex crystallized in triclinic space group $P\bar{1}$ with two dimer molecules per unit cell, each located on a different center of symmetry. A molecule of 2-methoxythiophene was also found in a general position. Solution and refinement were carried out as above. Fractional coordinates are given in the supplementary material and selected distances and angles in Table II.

X-ray Structural Determination of *cis*-$[(C_5Me_5)Rh(\mu\text{-}SC_4H_3OMe)]_2$. The data collection, solution, and refinement of this molecule proceeded as above, except that the complex crystallized in triclinic space group $P\bar{1}$ with two dimer molecules per unit cell (one full molecule lying in a general position). Solution and refinement were carried out as above. Fractional coordinates are given in the supplementary material and selected distances and angles in Table II.

Acknowledgment is made to the National Science Foundation (Grant CHE-9102318) for support of this work. W.D.J. also thanks NATO for a travel grant.

Supplementary Material Available: Tables of crystallographic data, including intramolecular distances and bond angles, positional parameters, anisotropic U values, and least-squares planes (11 pages); tables of observed and calculated structure factors (23 pages). Ordering information is given on any current masthead page.

(20) $R_1 = \{\sum||F_o| - |F_c||\}/\{\sum|F_o|\}$ and $R_2 = \{\sum w(|F_o| - |F_c|)^2\}^{1/2}/\{\sum wF_o^2\}$, where $w = [\sigma^2(F_o) + (\rho F_o^2)^2]^{1/2}$ for the non-Poisson contribution weighting scheme. The quantity minimized was $\sum w(|F_o| - |F_c|)^2$. Source of scattering factors f_o, f', f'': Cromer, D. T.; Waber, J. T. *International Tables for X-Ray Crystallography*; Kynoch Press: Birmingham, England, 1974; Vol. IV, Tables 2.2B and 2.3.1.